ARTICLE

Hispidulin-mediated inhibition of lung cancer progression through PI3K/AKT Signaling: A combined bioinformatic analysis and experimental investigation

Selvam Rajendiran · Sriram Prasath · Nithya Ramesh · Dhivya Murugesan · Ramadurai Murugan · Shobana Chandrasekar

Received: 1 February 2026 / Accepted: 1 April 2026

Abstract
Non-small cell lung cancer (NSCLC) continues to be one of the foremost causes of cancer-associated mortality globally, underscoring the critical need for novel therapeutic agents with broad, multi-targeted efficacy. In the present study, the anticancer potential of hispidulin, a naturally occurring prenylated flavonoid, was evaluated against NSCLC using an integrated strategy that combined network pharmacology, molecular docking, and in vitro validation. Network pharmacology analysis identified PI3K, AKT1, mTOR, and BCL2 as key hub targets, all of which play pivotal roles in regulating cell survival, proliferation, and resistance to apoptosis. Molecular docking studies revealed strong binding interactions between hispidulin and these core proteins, indicating its potential to directly modulate their activity. In vitro assays demonstrated dose- and time-dependent cytotoxic effects, with IC_{50} values of 129.63 µM at 24 h and 88.45 µM at 48 h. Morphological assessment by phase-contrast microscopy showed cellular shrinkage, while propidium iodide staining confirmed nuclear condensation and fragmentation. Elevated intracellular ROS levels detected by DCF-DA staining suggested the involvement of oxidative stress-mediated apoptotic pathways. Flow cytometric analysis further revealed G0/G1-phase cell cycle arrest and a significant increase in apoptotic cell populations following prolonged exposure to hispidulin. Consistent with these findings, quantitative RT-PCR analysis demonstrated significant downregulation of PI3K, AKT1, mTOR, and BCL2 transcripts, validating the molecular mechanism underlying hispidulin-induced cytotoxicity. Collectively, these results highlight hispidulin as a promising natural anticancer agent against NSCLC, exerting its effects through multi-targeted suppression of the PI3K/AKT/mTOR signaling axis and induction of apoptosis via ROS-mediated mechanisms.

Keywords Hispidulin · Lung cancer · Treatment · Diagnostics · Gene expression · Cell death

Introduction

Lung cancer is one of the most prevalent and deadly malignancies worldwide and remains a major public health challenge due to its high incidence, late diagnosis, and poor prognosis (Barta et al. 2019, Leiter et al. 2023). It is broadly classified into non-small cell lung cancer (NSCLC), which accounts for nearly 85% of cases, and small cell lung cancer (SCLC), known for its aggressive clinical course (Bade and Cruz 2020). The development and progression of lung cancer are driven by complex genetic and molecular alterations involving key oncogenic signaling pathways such as PI3K/AKT/mTOR, MAPK, EGFR, and apoptotic regulators including BCL-2 family proteins. Although conventional treatment modalities—such as surgery, chemotherapy, radiotherapy, targeted therapy, and immunotherapy—have improved patient outcomes, their effectiveness is often limited by drug resistance, systemic toxicity, high costs, and adverse side effects (Zafar et al. 2025, Schirrmacher 2019, Sen et al. 2024). These limitations underscore the need for safer, more effective therapeutic alternatives that can selectively target cancer cells while minimizing damage to normal tissues.

In recent years, phytocompounds derived from medicinal plants have gained significant attention as promising candidates in lung cancer management due to their structural diversity, multi-targeted mechanisms, and relatively low toxicity (Alrumaihi et al. 2025). Numerous natural compounds, including flavonoids, alkaloids, terpenoids, polyphenols, and coumarins, have demonstrated potent anticancer activities by modulating multiple signaling pathways involved in cell proliferation, apoptosis, metastasis, angiogenesis, and immune evasion (Situmorang et al. 2024). Phytochemicals such as curcumin, quercetin, resveratrol, luteolin, hispidulin, and epigallocatechin gallate (EGCG) have been shown to inhibit key oncogenic pathways like PI3K/AKT/mTOR and NF-κB, induce reactive oxygen species (ROS)-mediated apoptosis, arrest the cell cycle, and suppress epithelial–mesenchymal transition (EMT) in lung cancer models (Zughaibi et al. 2021, ul Islam et al. 2021). Moreover, phytocompounds have demonstrated the ability to sensitize cancer cells to conventional chemotherapeutic agents, thereby overcoming drug resistance and enhancing therapeutic efficacy. Owing to their multi-targeted action and favorable safety profiles, phytocompounds represent a valuable and emerging strategy in lung cancer treatment, either as standalone agents or as adjuvants to existing therapies, offering new avenues for the development of effective and less toxic anticancer interventions.

Hispidulin, a naturally derived flavonoid found in several medicinal plants, including Salvia officinalis, Artemisia species, and Clerodendrum species, has attracted increasing interest due to its wide range of pharmacological activities, particularly its anticancer properties (Patel and Patel 2017, Chaudhry et al. 2024). Chemically, hispidulin is classified as a flavone and contains hydroxyl and methoxy groups that contribute to its potent antioxidant capacity and biological activity. Its anticancer effects arise from the modulation of multiple molecular pathways, enabling selective targeting of cancer cells with minimal cytotoxicity to normal cells. Taken together, these multifaceted mechanisms position hispidulin as a promising natural anticancer compound, either as an independent therapeutic agent or in combination with existing cancer treatments, meriting further investigation through advanced preclinical and clinical studies (Ashaq et al. 2021). Despite these promising results, its pharmacological use has been limited by poor solubility and bioavailability, necessitating further mechanistic and therapeutic research.

In view of the pressing need for safer and more effective therapeutic options for NSCLC, along with the promising yet insufficiently explored anticancer potential of hispidulin, the present study aims to evaluate its therapeutic efficacy against NSCLC using an integrated bioinformatic and experimental approach. This research primarily focuses on assessing the ability of hispidulin to suppress key oncogenic signaling pathways, promote apoptotic cell death, and inhibit tumor progression. In addition, in silico ADME and drug-likeness analyses were conducted to predict its pharmacokinetic behavior and suitability for drug development. By combining computational predictions with in vitro validation, this study provides a comprehensive assessment of hispidulin as a potential therapeutic candidate for NSCLC, elucidating its underlying molecular mechanisms while highlighting its translational relevance.

Materials and methods

Network Pharmacology Analysis

A network pharmacology strategy was applied to elucidate the potential molecular targets and underlying pharmacological mechanisms of hispidulin in NSCLC. The canonical SMILES structure of hispidulin was retrieved from the PubChem database, and its putative protein targets were predicted using the SwissTargetPrediction and PharmMapper platforms. In parallel, NSCLC-related genes were compiled from multiple disease-associated databases, including the GeneCards database (Safran 2010). Common targets between hispidulin-associated proteins and NSCLC-related genes were identified using Venn diagram analysis, representing the potential therapeutic targets of hispidulin. These intersecting targets were subsequently imported into Cytoscape software to construct a drug–target–disease interaction network. Network topological parameters such as degree, betweenness centrality, and closeness centrality were analyzed to identify key hub genes that may play pivotal roles in mediating the anticancer effects of hispidulin.

Molecular Docking

Molecular docking analyses were performed to assess the binding interactions between hispidulin and key NSCLC-associated target proteins. The three-dimensional structure of hispidulin was obtained from the PubChem database and converted into PDB format using Open Babel, followed by energy minimization to achieve a stable conformation. The crystal structures of target proteins, including AKT1, BAX, PI3K, mTOR, BCL2, and GLUT2, were retrieved from the Protein Data Bank (PDB) (Burley et al. 2017). Protein structures were prepared by removing water molecules, adding polar hydrogen atoms, and assigning Kollman charges. Docking simulations were initially conducted using PyRx integrated with AutoDock Vina to predict binding affinities and optimal ligand–protein conformations. The resulting docking complexes were further analyzed and visualized using Discovery Studio Visualizer to examine key molecular interactions, such as hydrogen bonding, hydrophobic interactions, and interacting amino acid residues, thereby validating the binding stability and orientation of hispidulin with the selected targets.

Molecular dynamics (MD) simulation

Molecular dynamics (MD) simulations were performed using the GROMACS software package, with additional computational support provided through the WebGRO server (https://simlab.uams.edu/) (Burley et al. 2017, Eswaran et al. 2026, Seetharaman et al. 2025, Pushpanathan et al. 2025). The docked PI3K–hispidulin complex was separated into protein and hispidulin components for the simulation setup. Protein topology was generated using the AMBER99SB-ILDN force field within GROMACS, while ligand topology parameters were obtained via the PRODRG server. The individual topologies were then combined to reconstruct the complete receptor–ligand system. The complex was placed in a dodecahedral simulation box with a 1.0 nm buffer distance, solvated using the TIP3P water model, and neutralized by the addition of 0.15 M NaCl. MD simulations were carried out for 10 ns using the SFTP command-line interface on an Ubuntu platform. The results confirmed the structural stability of the protein–ligand complex under dynamic simulation conditions.

Pharmacokinetic Analysis

The pharmacokinetic characteristics and drug-likeness of hispidulin were assessed using the SwissADME web-based platform. The canonical SMILES representation of hispidulin was submitted to evaluate key absorption, distribution, metabolism, and excretion (ADME) parameters. Drug-likeness was examined based on established criteria, including Lipinski's Rule of Five, as well as the Ghose, Veber, and Egan filters. In addition, predictions

related to gastrointestinal absorption, blood–brain barrier permeability, aqueous solubility, and bioavailability were analyzed to determine the compound's suitability as a drug candidate. These in silico pharmacokinetic evaluations offered valuable insights into the potential of hispidulin for further advancement in preclinical and clinical drug development.

Cell Culture

The A549 human lung adenocarcinoma epithelial cell line (species: Homo sapiens; sex: male; tissue of origin: lung alveolar basal epithelium), 3T3-L1 (Mouse fibroblast cell line) were used in this study. The cell lines were obtained from the National Centre for Cell Science (NCCS), Pune, India, which supplies authenticated cell lines verified by morphological assessment, isoenzyme analysis, and short tandem repeat (STR) profiling. The official cell lines were A549 (ATCC® CCL-185™; RRID: CVCL_0023) and 3T3-L1 (ATCC® CL173™). The cells were certified by the supplier as free of bacterial, fungal, and mycoplasma contamination at the time of dispatch. In addition, routine in-house mycoplasma testing was conducted throughout the study to ensure continued sterility. Cells were maintained in Dulbecco's Modified Eagle Medium (DMEM; Himedia) supplemented with 10% fetal bovine serum (FBS), 1% penicillin–streptomycin, and 1% L-glutamine (Himedia). Cultures were incubated at 37 °C in a humidified 5% CO_2 atmosphere using a CO_2 incubator (Thermo Scientific). Cells were routinely subcultured using trypsin–EDTA (Himedia) upon reaching 70–80% confluence, and only cells in the logarithmic growth phase were utilised for all experimental procedures.

Cytotoxicity by MTT assay

The cytotoxic potential of hispidulin (SML0582, Merck) on A549 and mouse fibroblast, 3T3-L1 cells was determined using the MTT assay as previously described (Natarajan et al. 2025). Cells were seeded in 96-well plates at a density of 5×10^3 cells per well and allowed to adhere overnight. Following treatment with various concentrations of hispidulin (0–100 µM) for 24 and 48 h, 20 µL of MTT solution (5 mg/mL in PBS) was added to each well, and the plates were incubated for 4 h at 37 °C. The resulting formazan crystals were dissolved using 150 µL of DMSO (Himedia), and absorbance was measured at 570 nm using a microplate reader (Robonik, india). Cell viability was calculated relative to untreated control cells.

Nuclear Morphology Analysis (PI Staining)

Apoptotic nuclear alterations were assessed using PI staining (SRL). A549 cells were cultured on sterile coverslips in 6-well plates and exposed to hispidulin for 48 h of treatment. Following treatment, the cells were fixed with 4% paraformaldehyde, permeabilized using 0.1% Triton X-100, and stained with (10 mg/mL) for 10 min in the dark. The stained coverslips were mounted on glass slides with an antifade mounting medium, and nuclear morphology was observed under a fluorescence microscope (Olympus, Japan). Apoptotic cells were characterized by nuclear condensation and fragmentation, in contrast to the uniformly round nuclei observed in control cells.

Intracellular ROS Measurement (DCF-DA Staining)

Intracellular reactive oxygen species (ROS) production was evaluated using 2′,7′-dichlorofluorescin diacetate (DCF-DA, SRL). A549 cells were plated in 6-well plates and treated with hispidulin for 48 h. After treatment, cells were incubated with 10 µM DCF-DA prepared in serum-free medium for 30 min at 37 °C in the dark. The cells were then washed with PBS, and fluorescence was visualized using a fluorescence microscope at an excitation/emission wavelength of 485/530 nm (Natarajan et al. 2025). Enhanced green fluorescence intensity in treated cells indicated increased ROS generation compared with untreated control cells.

Cell Cycle and Cell Death Analysis by flow cytometry analysis

Flow cytometric analysis was performed to assess cell cycle progression and apoptosis. For cell cycle assessment, both hispidulin treated and untreated A549 cells were collected, washed with PBS, and fixed in 70% ethanol at −20 °C overnight. The fixed cells were subsequently washed, incubated with RNase A (50 µg/mL), and stained with propidium iodide (PI, 10 mg/mL) for 30 min at room temperature in the dark, as previously described (Velmurugan et al. 2025). DNA content was analyzed by flow cytometry, and the proportions of cells in the G0/G1, S, and G2/M phases were determined. For apoptosis analysis, cells were stained with Annexin V–FITC and PI according to the manufacturer's instructions and analyzed by flow cytometry to discriminate early apoptotic, late apoptotic, and necrotic cell populations in BC cytflow instrument.

Gene Expression Analysis (RT-PCR)

Quantitative expression analysis of apoptosis- and proliferation-associated genes was conducted using reverse transcription polymerase chain reaction (RT-PCR), as previously described (Natarajan et al. 2024). Total RNA was isolated from treated and untreated A549 cells using TRIzol reagent, and RNA purity was assessed by determining the 260/280 nm absorbance ratio. Complementary DNA (cDNA) was synthesized from 1 µg of total RNA using a reverse transcription kit. RT-PCR was performed with gene-specific primers for BAX, BCL2, CASPASE-3, AKT1, mTOR, PI3K, and β-actin (Table 1). Amplification was carried out in a thermal cycler (Biorad, CFX9 system) under optimized cycling conditions. Relative gene expression levels were calculated using the $2^{-}\Delta\Delta Ct$ method, and fold changes were compared between hispidulin-treated and control groups.

Statistical analysis

In this study, statistical analyses were performed using the R programming language, a widely used platform for statistical computing and data analysis. Differential gene expression between paired normal and tumor tissues from the TCGA dataset was assessed using Student's paired t-test. Statistical significance was defined as $*p<0.05$, $**p<0.01$, $***p<0.001$, and $****p<0.0001$. All experiments were conducted in independent triplicate (mean ± SD) using Graphpad Prism software.

Table 1 RT-PCR list

Gene(s)	Primer 5'−3'
AKT1	F-TTCTGCAGCTATGCGCAATGTG R-TGGCCAGCATACCATAGTGAGGTT
Bcl-2	F-GACGCTTTGCCACGGTGGTG R-GGGGCAGGCATGTTGACTTCAC
PI3K	F-GGTTGTCTGTCAATCGGTGACTGT R-GAACTGCAGTGCACCTTTCAAGC
MTOR	F-ACTGATGGAGTCCGAAATGC R-TCATCCGATCCTTCATCCTC
BAX	F-TTCTGACGGCAACTTCAACTG R-TGAGGAGTCTCACCCAACCA
CASP3	F- CTTCAGTGGTGGACATGACG R- TCAACAATTTGAGGCTGCTG
β-actin	F-AACAAGATGAGATTGGCA R-AGTGGGGTGGCTTTTAGGAT

Results

Network Pharmacology and Target Identification

Network pharmacology analysis integrating the GeneCards and CTD databases identified a panel of hispidulin-associated targets relevant to NSCLC (Fig. 1A). Intersection analysis revealed 20 overlapping targets, among which BCL2, BAX, CASP3, AKT1, PI3K, and mTOR emerged as key hub genes (Fig. 1B and C). These targets are critically involved in the regulation of apoptosis, cell survival, proliferation, and drug resistance. Construction of the protein–protein interaction (PPI) network further highlighted their central roles, as they exhibited high connectivity, indicating that hispidulin may exert its anticancer effects primarily through modulation of the PI3K/AKT/mTOR signaling pathway and apoptosis-related regulators such as BCL2. Collectively, these findings provide a strong rationale for exploring hispidulin as a multitarget therapeutic candidate capable of suppressing oncogenic signaling in NSCLC.

Molecular Docking Validation

Molecular docking analysis demonstrated that hispidulin exhibits strong binding affinity toward BCL2, AKT1, PI3K, GLUT2 BAX, and mTOR. The docking simulations revealed stable hydrogen bonding and hydrophobic interactions within the respective active sites, suggesting the potential for direct inhibition of these target proteins. These results are consistent with the network pharmacology findings and indicate that hispidulin simultaneously targets key survival-related proteins (AKT1, PI3K, and mTOR) and the anti-apoptotic protein BCL2 (Fig. 2; Table 2). Collectively, these observations support a dual mechanistic role of hispidulin in suppressing cellular proliferation while promoting apoptosis in NSCLC.

Representative binding conformations illustrating the stable interactions of hispidulin with BCL-2, PI3K, AKT1, and mTOR. Hydrogen bonding and hydrophobic interactions suggest hispidulin fits into the active sites of these proteins, supporting its inhibitory potential against anti-apoptotic and pro-survival pathways.

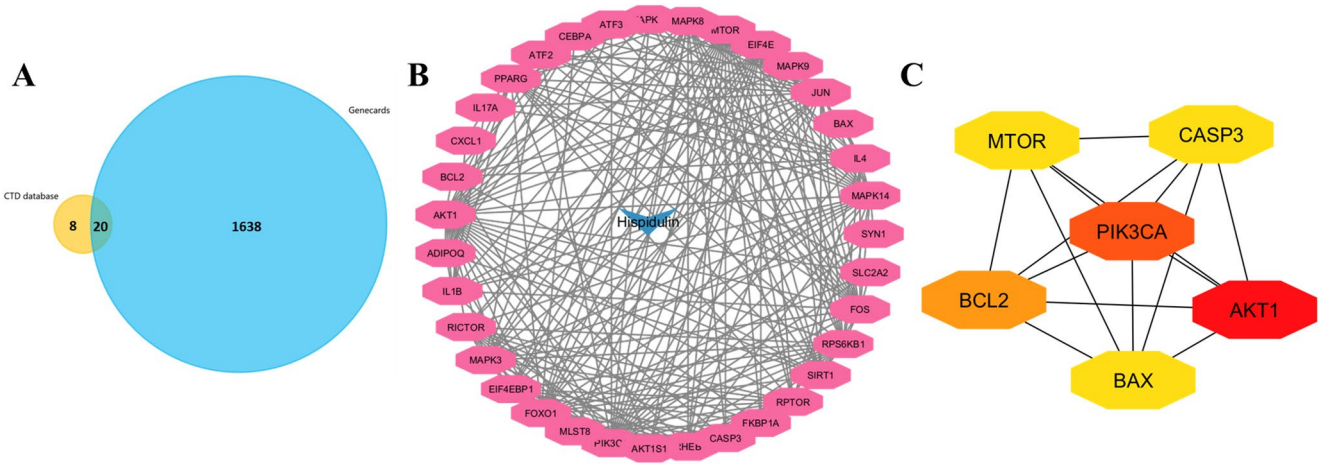

Fig. 1 Network pharmacology-based identification of hispidulin targets in NSCLC. (A) Venn diagram showing the intersection of hispidulin-associated targets retrieved from GeneCards and CTD databases, which results in 20 common genes.(B) Protein–protein interaction (PPI) network created using Cytoscape reveals strong connections among the identified targets, emphasizing BCL2, AKT1, BAX, CASP3, PI3K, and mTOR as key hub genes. (C) Schematic representation of hispidulin's core targets (BCL2, BAX, CASP3, AKT1, PI3K, and mTOR), indicating their potential roles in regulating apoptosis and proliferation in NSCLC

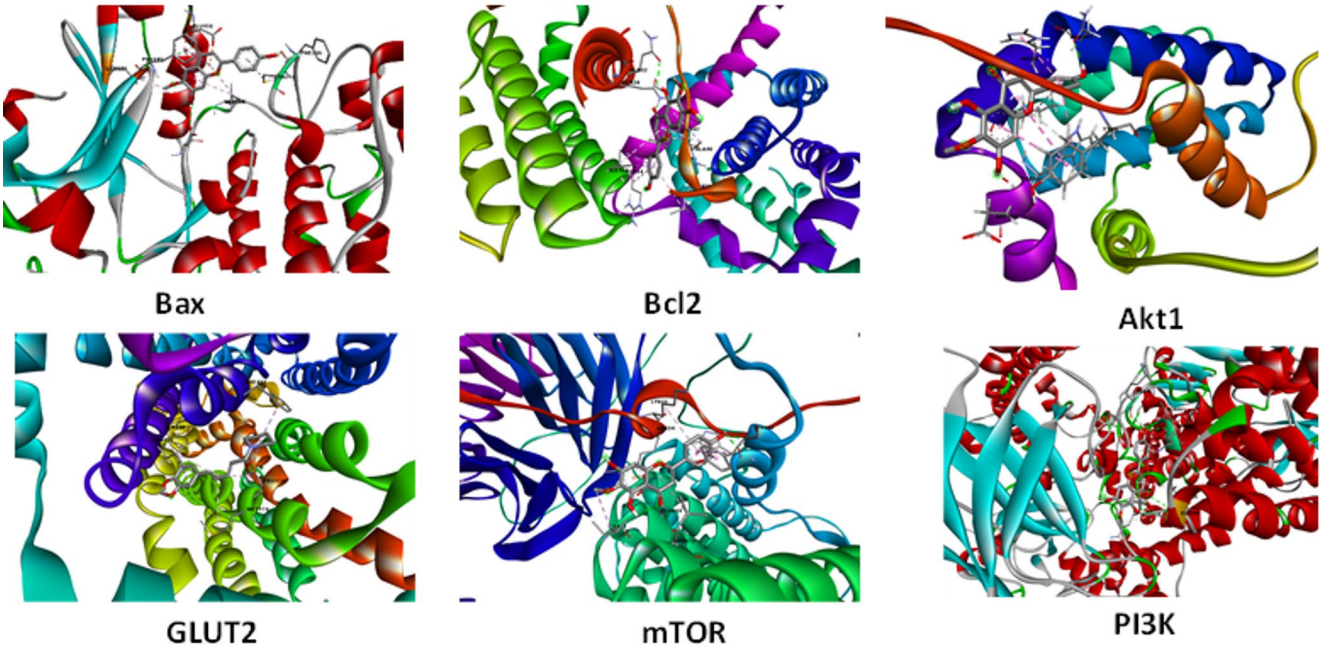

Fig. 2 Molecular docking of hispidulin with core target proteins

Table 2 Molecular docking binding scores

Compound	Protein(s)	Binding energy (Kcal/mol)	Amino acid binds with H bonds
Hispidulin (CID: 5281628)	Bax	−7.8	GLN32, GLN28
	BCl2	−7.5	ASN182
	AKT1	−7.5	PHE310
	GLUT2	−8.9	GLY170, TRP420
	mTOR	−7.7	TRP962, TYR966, ARG34
	PI3K	−8.5	GLU135, GLN682, LYS678, SER681, LEU645

Molecular dynamics

Moreover, the 10 ns molecular dynamics simulation of the PI3K–hispidulin complex performed using GROMACS indicates a high degree of structural stability throughout the simulation period. The RMSD profile shows an initial rise during the equilibration phase, followed by stabilization around ~0.28–0.34 nm, suggesting that the protein–ligand complex rapidly reached equilibrium and remained conformationally stable without significant structural drift. This stable RMSD plateau hispidulin's docked binding mode within the PI3K active site. Additionally, the RMSF analysis shows generally low residue-level fluctuations across the protein, with only moderate flexibility in loop regions, which is typical and does not compromise the overall integrity of the complex. Importantly, residues within the binding region showed minimal fluctuations, indicating strong, persistent interactions between PI3K and hispidulin as shown in (Fig. 3). Collectively, these results confirm that the PI3K–hispidulin complex is dynamically stable over the 10 ns simulation, supporting the reliability of the docking results and suggesting favorable binding under physiological-like conditions.

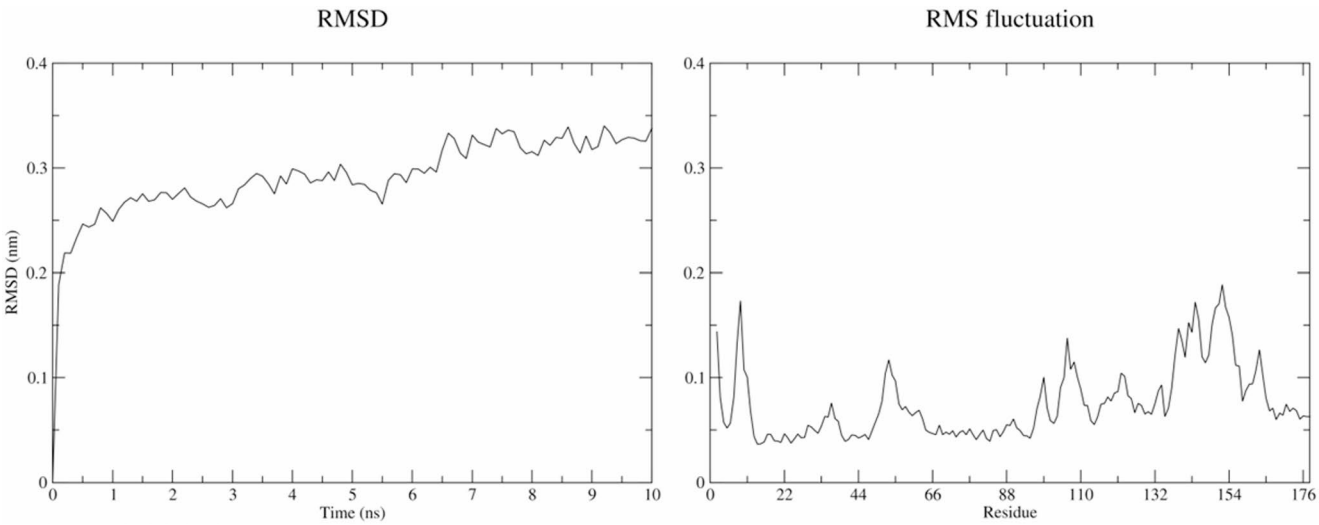

Fig. 3 Molecular dynamics. RMSD and RMS fluctuation plots show the binding interaction between the PI3K-Hispidulin complex over 10 ns using GROMACS software

Pharmacokinetics by the ADME property

The in silico ADME–T evaluation of hispidulin indicates a favorable pharmacokinetic and drug-likeness profile. Hispidulin has a molecular formula of $C_{16}H_{12}O_6$ with a molecular weight of 300.26 Da, well within the acceptable range for orally active small molecules, and contains 22 heavy atoms, of which 16 are aromatic, reflecting a predominantly aromatic scaffold with a low fraction of sp^3 carbons (0.06). The compound exhibits a topological polar surface area (TPSA) of 100.13 $Å^2$, which supports good intestinal absorption and is consistent with its predicted high gastrointestinal (GI) absorption. Lipophilicity values were moderate, with a consensus LogP of 2.12 (iLOGP 2.27, XLOGP3 2.99, WLOGP 2.59, Silicos-IT LogP 2.55), suggesting an appropriate balance between aqueous solubility and membrane permeability.

Solubility predictions classified hispidulin as soluble to moderately soluble, with ESOL LogS of −3.99 (0.0306 mg/mL), Ali LogS of −4.76 (0.00526 mg/mL), and Silicos-IT LogSw of −4.52 (0.00907 mg/mL), indicating acceptable solubility for oral administration. Hispidulin is predicted to be non-permeant to the blood–brain barrier (BBB) and not a P-glycoprotein substrate, reducing the likelihood of central nervous system toxicity and efflux-mediated loss of bioavailability. In terms of metabolism, the compound is predicted to inhibit CYP1A2, CYP2D6, and CYP3A4, suggesting a potential for drug–drug interactions, while showing no inhibitory effects on CYP2C19 or CYP2C9. The predicted skin permeability (log Kp = −6.01 cm/s) indicates low transdermal absorption.

Importantly, hispidulin satisfies all major drug-likeness filters, including Lipinski, Ghose, Veber, Egan, and Muegge rules, with no violations, and displays a favorable bioavailability score of 0.55 (Table 3). Additionally, no PAINS or Brenk structural alerts were identified, and no lead-likeness violations were observed, supporting its suitability as a drug-like candidate. Overall, the ADME–T profile suggests that hispidulin possesses favorable oral absorption, acceptable solubility, and good drug-likeness, reinforcing its potential as a promising small-molecule therapeutic agent.

Cytotoxicity Assay

The MTT assay revealed that hispidulin significantly reduced A549 cell viability in both a concentration- and time-dependent manner. The half-maximal inhibitory concentration (IC_{50}) was determined to be 129.63 µM at 24 h and 88.45 µM at 48 h, indicating enhanced cytotoxicity with prolonged exposure (Fig. 4A). Consistent

Table 3 ADME-T property

Molecule	Hispidulin	Consensus Log *P*	2.12
Canonical SMILES	COc1c(O)cc2c(c1O)c(=O)cc(o2)c1ccc(cc1)O	ESOL Log S	−3.99
Formula	C16H12O6	ESOL Solubility (mg/ml)	0.0306
MW	300.26	ESOL Solubility (mol/l)	0.000102
#Heavy atoms	22	ESOL Class	Soluble
#Aromatic heavy atoms	16	Ali Log S	−4.76
Fraction Csp3	0.06	Ali Solubility (mg/ml)	0.00526
#Rotatable bonds	2	Ali Solubility (mol/l)	1.75E-05
#H-bond acceptors	6	Ali Class	Moderately soluble
#H-bond donors	3	Silicos-IT LogSw	−4.52
MR	80.48	Silicos-IT Solubility (mg/ml)	0.00907
TPSA	100.13	Silicos-IT Solubility (mol/l)	3.02E-05
iLOGP	2.27	Silicos-IT class	Moderately soluble
XLOGP3	2.99	GI absorption	High
WLOGP	2.59	BBB permeant	No
MLOGP	0.22	Pgp substrate	No
Silicos-IT Log P	2.55	CYP1A2 inhibitor	Yes
Lipinski #violations	0	CYP2C19 inhibitor	No
Ghose #violations	0	CYP2C9 inhibitor	No
Veber #violations	0	CYP2D6 inhibitor	Yes
Egan #violations	0	CYP3A4 inhibitor	Yes
Muegge #violations	0	log Kp (cm/s)	−6.01
Bioavailability Score	0.55	Brenk #alerts	0
PAINS #alerts	0	Leadlikeness #violations	0

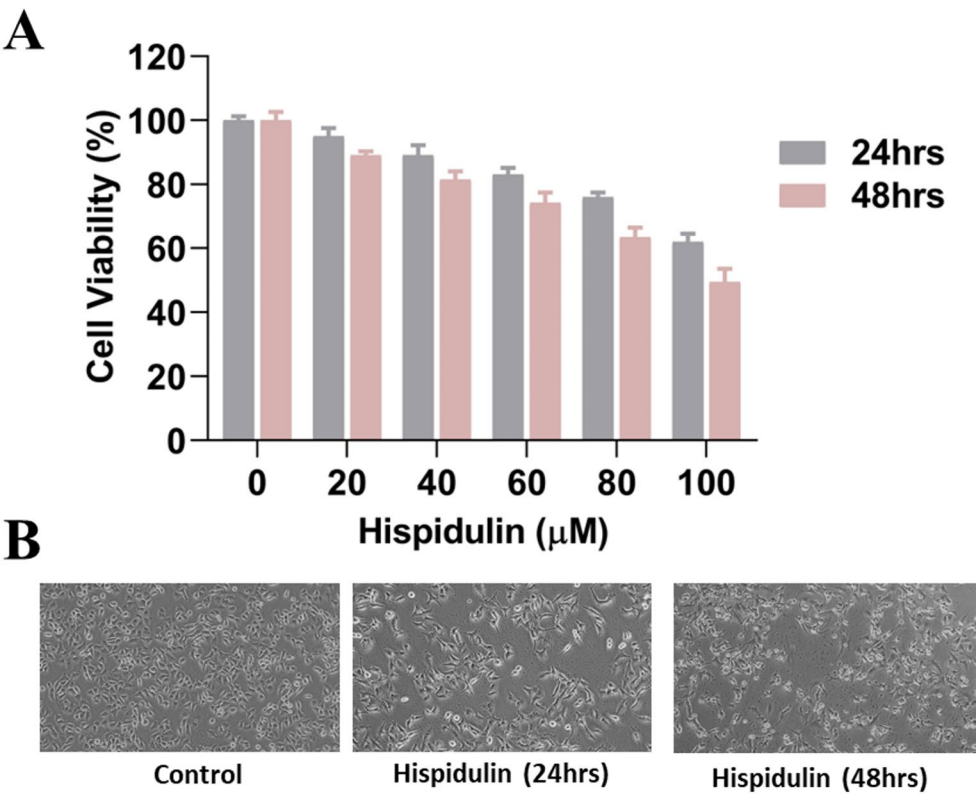

Fig. 4 Cytotoxic effects of Hispidulin on A549 cells. (A) MTT assay showing dose- and time-dependent reduction in cell viability following hispidulin treatment at 24 h and 48 h. IC_{50} values were 129.63 µM at 24 h and 88.45 µM at 48 h. (B) Representative phase-contrast micrographs demonstrate reduced confluency, morphological shrinkage, and detachment in the treated groups compared to the control, consistent with cytotoxic and apoptotic effects

with these findings, phase-contrast microscopic examination showed marked morphological alterations in treated cells, including reduced cell density, loss of cell–cell adhesion, and characteristic apoptotic shrinkage at higher concentrations of hispidulin (Fig. 4B). Moreover, biocompatibility of hispidulin (0–100µM) treated in 3T3-L1 cells shows no toxic effects (Sup. Figure 1). Collectively, these results confirm the cytotoxic potency of hispidulin against A549 cells and provided a basis for selecting IC_{50} concentrations for subsequent mechanistic analyses.

Nuclear and Oxidative Stress Studies

PI staining was used to assess nuclear morphology and confirm apoptosis at the cellular level. In untreated A549 control cells, nuclei were intact, round, and uniformly stained, indicating normal nuclear architecture and chromatin organization. In contrast, cells exposed to hispidulin for 48 h exhibited early apoptotic features, including chromatin condensation and nuclear margination. Following 48 h of treatment, apoptotic changes were more pronounced, with evident nuclear fragmentation and the formation of apoptotic bodies (Fig. 5A). These observations

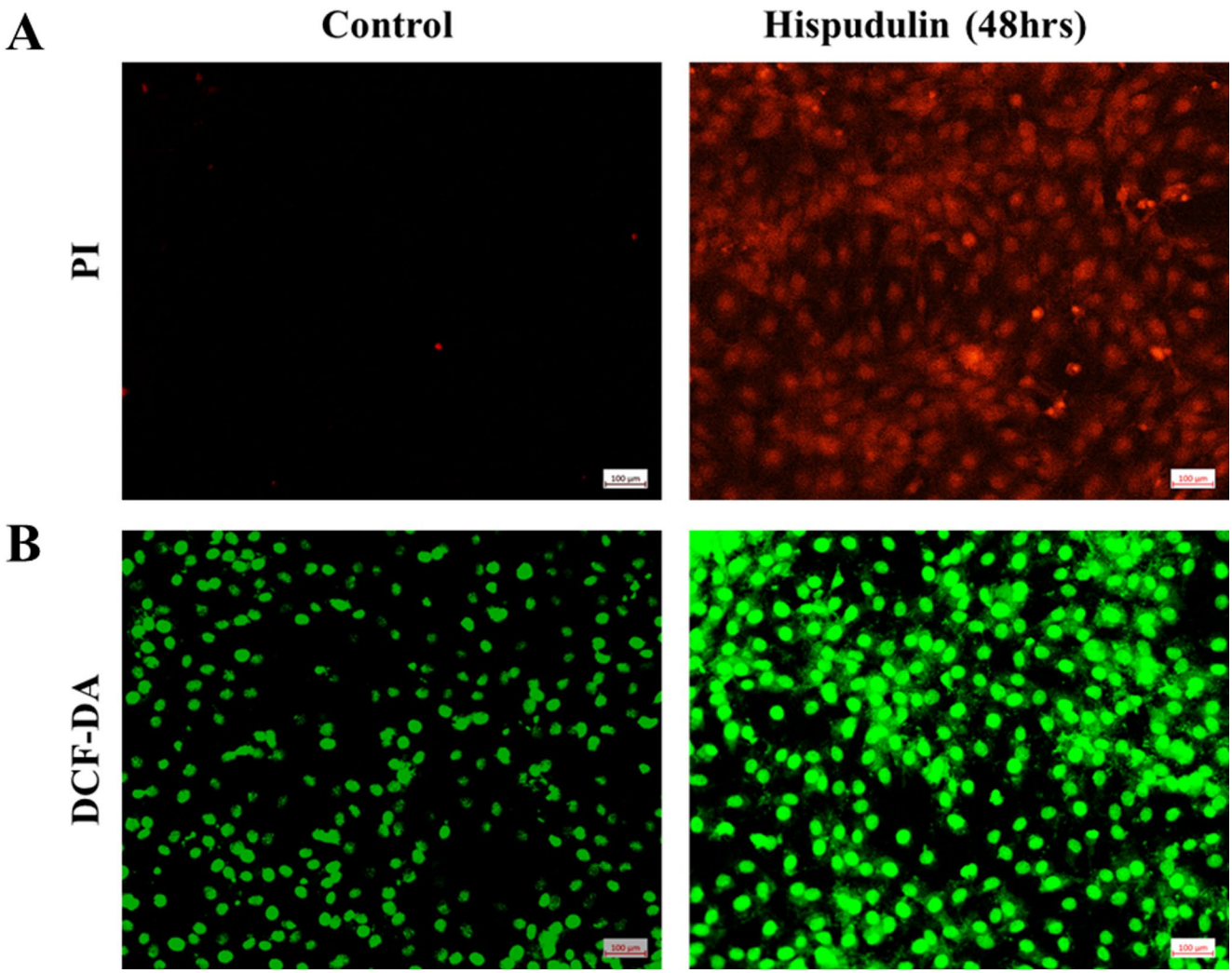

Fig. 5 Nuclear morphology and ROS generation upon hispidulin treatment. (A) PI staining shows intact nuclei in the control group, while hispidulin-treated cells (48 h) display nuclear condensation and fragmentation, indicative of apoptosis. (B) DCF-DA staining demonstrates a marked increase in green fluorescence in hispidulin-treated cells, reflecting elevated intracellular ROS levels compared to control. These results suggest ROS-mediated apoptotic induction

demonstrate that hispidulin induces apoptosis in a time-dependent manner, supporting its role in activating intrinsic apoptotic pathways in A549 cells.

Intracellular reactive oxygen species (ROS) generation in hispidulin-treated NSCLC cells was assessed using DCF-DA staining. Control cells displayed minimal fluorescence, corresponding to basal ROS levels required for normal cellular function. In contrast, treatment with hispidulin for 48 h resulted in a noticeable increase in green fluorescence, indicating elevated ROS production. This effect was further intensified after 48 h, with a marked increase in fluorescence intensity, reflecting substantial ROS accumulation in A549 cells (Fig. 5B). Excessive ROS generation can induce oxidative damage to cellular macromolecules and trigger apoptotic signaling pathways. Collectively, these findings suggest that hispidulin promotes oxidative stress, potentially leading to mitochondrial dysfunction, cytochrome c release, and subsequent activation of caspase-dependent apoptosis.

Cell Cycle Analysis and Apoptosis Induction

Flow cytometric analysis revealed that hispidulin treatment induced a pronounced cell cycle arrest in A549 cells at the G0/G1 phase. In untreated control cells, the distribution of cells across the G0/G1, S, and G2/M phases was relatively balanced, reflecting normal proliferative activity. This effect became more prominent after 48 h, with a substantial increase in the G0/G1 population and a corresponding decline in DNA synthesis and mitotic progression (Fig. 6A). These findings indicate that hispidulin effectively disrupts cell cycle progression, likely by inhibiting critical checkpoint regulators, thereby preventing entry into the DNA replication phase.

To further validate the cytotoxic effects of hispidulin, apoptosis was evaluated using Annexin V/PI staining. Control cells predominantly remained viable, with minimal apoptotic populations, consistent with normal cellular homeostasis. After 48 h, both early and late apoptotic populations were markedly elevated, indicating progression toward irreversible cell death (Fig. 6B). Notably, the proportion of necrotic cells remained low throughout the treatment period, suggesting that hispidulin predominantly induces programmed cell death rather than necrosis, a desirable feature for minimizing inflammatory responses in anticancer therapy.

RT-PCR Gene Expression Analysis

RT-PCR analysis revealed that 48-hour hispidulin treatment markedly modulated the expression of apoptosis- and survival-related genes in A549 cells. Pro-apoptotic BAX expression was significantly upregulated compared with the control, indicating activation of apoptotic signaling. In contrast, the anti-apoptotic gene BCL2 was significantly downregulated, resulting in a favorable shift in the BAX/BCL2 ratio toward apoptosis. Consistent with inhibition of oncogenic survival pathways, key components of the PI3K/AKT/mTOR axis—PI3K, AKT1, and mTOR—showed a significant reduction in mRNA expression following hispidulin exposure. Additionally, GLUT2 expression was significantly reduced, further confirming activation of the execution phase of metabolic reprogramming (Fig. 7). Overall, these findings demonstrate that hispidulin induces apoptosis in A549 cells by upregulating pro-apoptotic and caspase genes while suppressing PI3K/AKT/mTOR-mediated survival signaling, supporting its multi-target anticancer potential after 48 h of treatment.

Discussion

The present study comprehensively evaluated the therapeutic potential of hispidulin against non-small cell lung cancer (NSCLC) using an integrated approach that combined network pharmacology, molecular docking, and ADME profiling. This multi-layered computational strategy enabled a systematic understanding of hispidulin's molecular targets, associated signaling pathways, and pharmacokinetic characteristics, underscoring its potential as a phytotherapeutic candidate for lung cancer management. Network pharmacology analysis identified 13 overlapping hispidulin-associated targets relevant to NSCLC, including key oncogenic regulators such as BCL2,

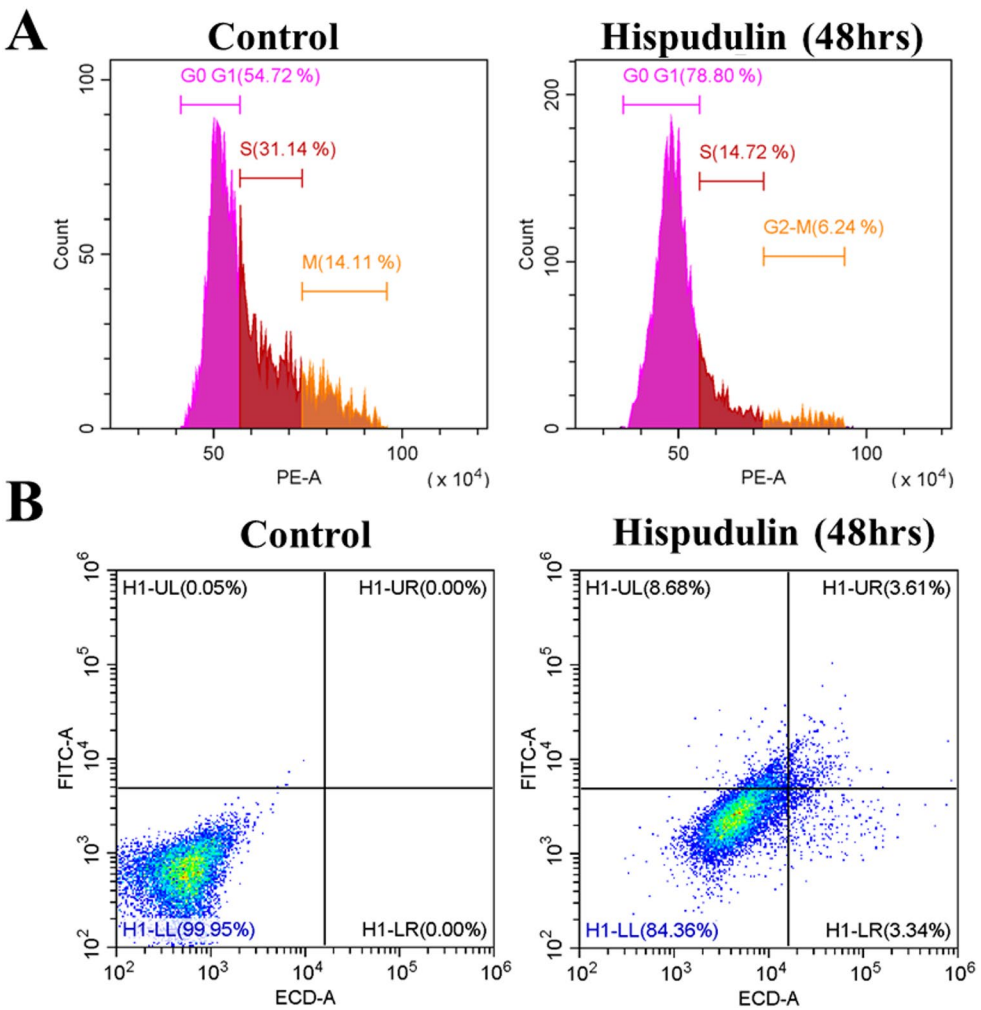

Fig. 6 Effect of hispidulin on Cell Cycle Progression and Apoptosis (A) Flow cytometry histograms display cell cycle distribution in control and 48 h hispidulin-treated groups. Quantitative analysis reveals a significant accumulation of cells in the G0/G1 phase, with a corresponding decrease in the S and M phases, confirming hispidulin-induced cell cycle arrest at the G0/G1 phase 48 h of hispidulin treatment compared to control. (B) Quantitative analysis confirms a time-dependent increase in apoptotic cells, accompanied by a notable reduction in live cell populations, demonstrating hispidulin-triggered apoptotic cell death

AKT1, PI3K, and mTOR, which are critically involved in apoptosis, cell survival, proliferation, and therapeutic resistance. Protein–protein interaction (PPI) network analysis further highlighted these molecules as central hub nodes, indicating that the anticancer activity of hispidulin is mediated through coordinated modulation of survival and apoptotic signaling networks.

Importantly, the PI3K/AKT/mTOR signaling axis emerged as a dominant pathway, consistent with its well-established role in NSCLC development, progression, and drug resistance (Wang et al. 2023, Jiang et al. 2020). Concurrent targeting of this pathway, along with downregulation of the anti-apoptotic protein BCL2, suggests a dual mechanism of action, involving suppression of tumour growth and induction of apoptosis. These observations were further supported by functional enrichment analyses, as KEGG and Reactome pathways were significantly enriched for PI3K/AKT, mTOR, apoptosis, EGFR, and NSCLC-related signaling pathways, reinforcing the biological relevance of the identified targets. Molecular docking analysis substantiated the network pharmacology findings by demonstrating strong binding affinities of hispidulin toward BCL2, AKT1, PI3K, and mTOR. The presence of stable hydrogen bonds and hydrophobic interactions within the active sites of these proteins suggests a high probability of functional inhibition. The concordance between docking results and network analysis highlights hispidulin's potential as a multi-target agent capable of exerting both pro-apoptotic and anti-proliferative effects in NSCLC.

The present study provides a comprehensive evaluation of the anticancer potential of hispidulin against non-small cell lung cancer (NSCLC) through an integrated framework combining in silico ADME–T profiling with in

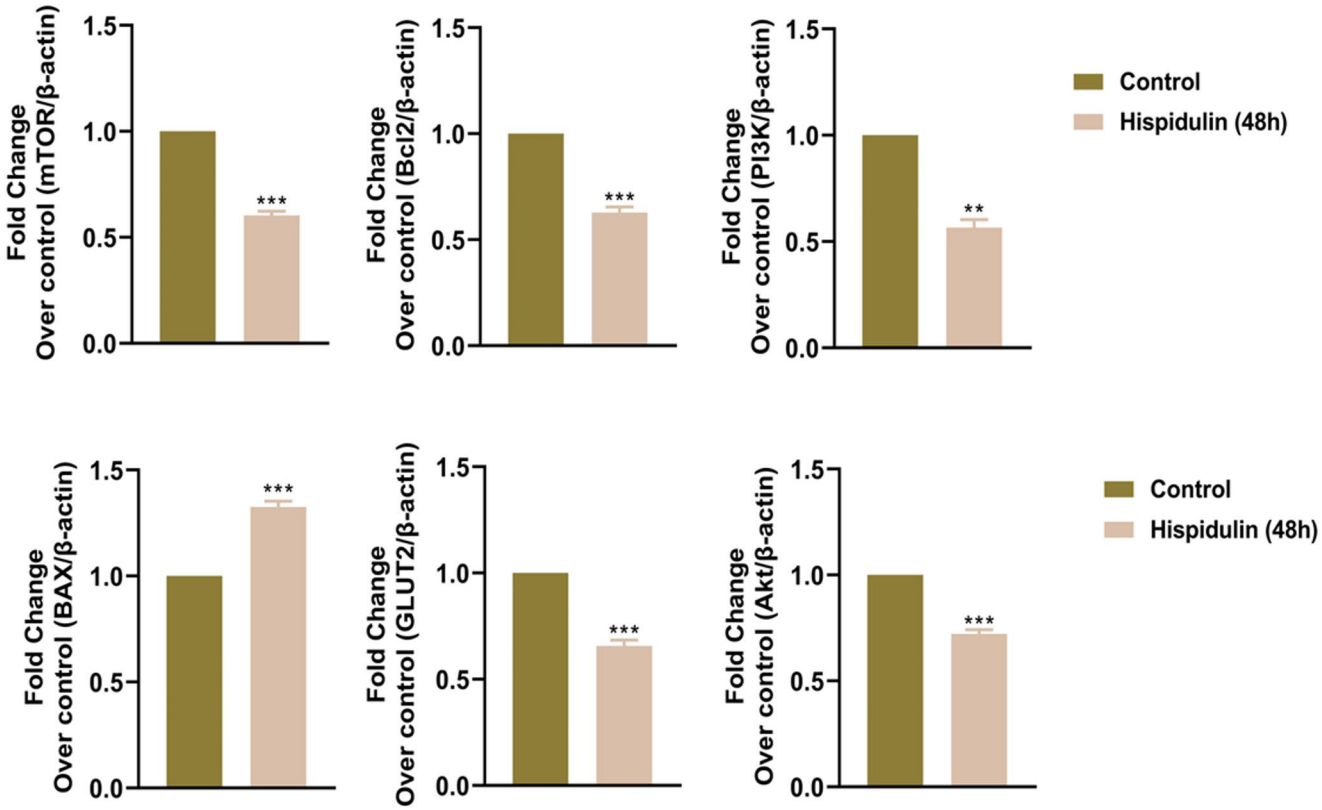

Fig. 7 RT-PCR validation of hispidulin-mediated gene regulation in A549 cells. Quantitative RT-PCR analysis of A549 cells treated with hispidulin for 48 h shows significant downregulation of PI3K, BCL2, AKT1, and mTOR compared to untreated controls. These results confirm that hispidulin exerts its anticancer effects by inhibiting PI3K/AKT/mTOR signaling and BCL2-mediated anti-apoptotic defense, promoting apoptosis in a time-dependent manner. Statistical significance at $*p<0.05$, $**p<0.001$, $***p<0.0001$

vitro functional validation in A549 cells (Citi 2017). The findings collectively demonstrate that hispidulin exerts multi-faceted anticancer effects by suppressing cell proliferation, inducing oxidative stress–mediated apoptosis, arresting cell cycle progression, and modulating key oncogenic signaling pathways, particularly the PI3K/AKT/mTOR axis.

In silico ADME–T analysis revealed that hispidulin possesses favorable drug-like and pharmacokinetic properties, supporting its suitability as an orally active small molecule (Adamu et al. 2023, Shakoor et al. 2024, Silva et al. 2023). Its molecular weight, moderate lipophilicity, and optimal topological polar surface area are consistent with efficient gastrointestinal absorption, which was further supported by predicted high GI permeability. Importantly, hispidulin satisfied all major drug-likeness filters, including Lipinski, Ghose, Veber, Egan, and Muegge rules, with no PAINS or Brenk alerts, suggesting a low likelihood of nonspecific toxicity or assay interference. Although moderate CYP inhibition was predicted, indicating a potential for drug–drug interactions, the overall ADME–T profile supports the feasibility of further preclinical development. These computational insights provide a strong rationale for the experimental validation of hispidulin's anticancer activity (Ashaq 2021).

Consistent with its favorable pharmacokinetic profile, hispidulin exhibited significant cytotoxic effects against A549 cells in a dose- and time-dependent manner, as demonstrated by the MTT assay (Cummings and Schnellmann 2021). The progressive reduction in IC_{50} values from 24 to 48 h indicates enhanced cytotoxic efficacy with prolonged exposure, suggesting sustained intracellular activity. Morphological assessment further corroborated these findings, revealing hallmark apoptotic features, including reduced cell density, loss of adhesion, and cellular shrinkage. Although the IC_{50} values observed in this study fall within the high micromolar range (129µM for 24

h and 88 µM for 48 h), such concentrations are not uncommon for phytochemicals evaluated in vitro analysis. Importantly, in vitro IC_{50} values do not directly reflect achievable plasma concentrations in vivo, as factors such as absorption, metabolic activation, tissue accumulation, and synergistic interactions can substantially influence biological activity. Several natural compounds exhibit limited standalone potency but exert significant anticancer effects in vivo through pathway modulation, chemo sensitization, or long-term exposure. Furthermore, formulation strategies, structural optimization, and combination approaches may enhance bioavailability and therapeutic efficacy.

Apoptosis induction was further validated at the nuclear level using PI/DAPI staining (Wu 2018). These nuclear alterations are characteristic of intrinsic apoptotic pathways and suggest mitochondrial involvement. Consistent with this hypothesis, DCF-DA staining revealed a substantial increase in intracellular reactive oxygen species (ROS) levels following hispidulin treatment. Elevated ROS levels are known to disrupt mitochondrial membrane potential, promote cytochrome c release, and activate downstream caspase cascades. Thus, the observed oxidative stress likely acts as a critical upstream trigger for hispidulin-induced apoptosis in NSCLC cells.

Flow cytometric analysis further demonstrated that hispidulin effectively disrupts cell cycle progression by inducing a robust arrest at the G0/G1 phase. The accumulation of cells in G0/G1, accompanied by a marked reduction in S and G2/M populations, indicates inhibition of DNA synthesis and mitotic entry. Such cell cycle arrest is a well-established anticancer mechanism, as it limits uncontrolled proliferation and sensitizes cancer cells to apoptotic signaling. Importantly, Annexin V/PI staining confirmed that hispidulin-induced growth inhibition was predominantly mediated by apoptosis rather than necrosis, as evidenced by a significant increase in early- and late-apoptotic populations, with minimal necrotic cell death (Dai, Lv et al. 2020). Naringenin effectively inhibits breast cancer cell growth and migration by causing S-phase arrest, inducing apoptosis, and activating pro-apoptotic autophagy, underscoring its therapeutic promise (Mir 2025). This review emphasizes flavonoids as affordable anticancer agents capable of overcoming drug resistance through regulation of oxidative stress, immune modulation, metastasis, and apoptosis/autophagy (Mir et al. 2024). Additionally, it outlines the dysregulation of mTOR signaling in cancer, detailing the roles of mTORC1 and mTORC2 and recent advances in mTOR inhibitors as key strategies for targeting tumor growth, metabolism, apoptosis, and autophagy (Mir 2023). Furthermore, lung cancer therapies and highlights phytochemicals as promising anticancer agents. It critically evaluates in vitro, in vivo, and clinical evidence, focusing on their ability to modulate key signaling pathways, apoptosis, oxidative stress, angiogenesis, and cell cycle regulation (Choudhary et al. 2023). Additionally, the review emphasizes nanoparticle-based drug delivery systems as effective strategies to overcome bioavailability limitations of phytocompounds (Fatima 2022). By enhancing targeted delivery, stability, and therapeutic efficacy while reducing systemic toxicity, nanotechnology-integrated phytoconstituents offer a viable and innovative approach for improved lung cancer management (Siddiquee et al. 2024). This is particularly desirable in anticancer therapy, as apoptosis minimizes inflammatory responses and collateral tissue damage. At the molecular level, RT-PCR analysis provided mechanistic insights into the pathways underlying hispidulin's anticancer effects. Treatment resulted in significant upregulation of the pro-apoptotic gene BAX and downregulation of the anti-apoptotic gene BCL2, thereby shifting the BAX/BCL2 ratio in favor of apoptosis. A key limitation of this study is the absence of Western blot validation of PI3K, AKT, mTOR, BCL2, and BAX, which precludes direct confirmation of pathway modulation. Future studies incorporating protein-level analyses are necessary to substantiate the proposed molecular mechanisms and strengthen the translational relevance of the findings. Concurrent suppression of PI3K, AKT1, and mTOR expression further highlights the inhibition of a central oncogenic survival pathway frequently dysregulated in NSCLC. Additionally, reduced GLUT2 expression suggests interference with cancer-associated metabolic reprogramming, further contributing to growth inhibition and apoptotic sensitization. Together, these molecular changes confirm that hispidulin exerts its effects through coordinated modulation of apoptotic, survival, and metabolic signaling networks.

Conclusion and future directions

Overall, this study shows that hispidulin exhibits potent anticancer effects against non-small cell lung cancer by targeting key oncogenic pathways involved in cell proliferation, survival, and apoptosis. Network pharmacology and molecular docking identified PI3K, AKT1, mTOR, and BCL2 as major targets, which were validated by RT-PCR. Functional assays demonstrated that hispidulin induces ROS generation, oxidative stress, G0/G1 cell cycle arrest, and apoptosis. Cytotoxicity, morphological, flow cytometry, and gene expression analyses collectively confirm its growth-inhibitory and pro-apoptotic effects. These findings support hispidulin as a promising multitargeted natural anticancer agent, warranting further protein-level validation and in vivo studies to enhance translational relevance.

Supplementary Information The online version contains supplementary material available at https://doi.org/10.1007/s10616-026-00958-0.

Author contributions Selvam Rajendiran, Sriram Prasath, Nithya Ramesh: Validation, Writing – review & editing. Dhivya Murugesan & Ramadurai Murugan: Data curation, Formal analysis, Investigation, Methodology, Writing – review & editing. Shobana Chandrasekar & Selvam Rajendiran: Conceptualization, Data curation, Writing – original draft.

Funding information No financial support was obtained for the research.

Data availability No datasets were generated or analysed during the current study.

Declarations

Competing interests The authors state that they have no known competing financial interests or personal relationships that could have influenced the work reported in this paper.

References

Adamu UM, Renggasamy R, Stanslas J, Razis AFA, Fauzi FM, Mulyani SWM, Ramasamy R (2023) In-silico prediction analysis of polyphenolic contents of ethanolic extract of *Moringa oleifera* leaves. Malaysian Journal of Medicine & Health Sciences. https://doi.org/10.47836/mjmhs.19.s16.3

Alrumaihi F, Rahmani AH, Prabhu SV, Kumar V, Anwar S (2025) The role of plant-derived natural products as a regulator of the tyrosine kinase pathway in the management of lung cancer. Curr Issues Mol Biol 47(7):498

Ashaq A, Maqbool MF, Maryam A, Khan M, Shakir HA, Irfan M, Ma T (2021) Hispidulin: A novel natural compound with therapeutic potential against human cancers. Phytother Res 35(2):771–789

Ashaq, A., Maqbool, M. F., Maryam, A., Khan, M., Shakir, H. A., Irfan, M., … Ma, T.(2021). Hispidulin: A novel natural compound with therapeutic potential against human cancers. Phytotherapy Research, 35(2), 771–789.

Bade BC, Cruz CSD (2020) Lung cancer 2020: epidemiology, etiology, and prevention. Clin Chest Med 41(1):1–24

Barta JA, Powell CA, Wisnivesky JP (2019) Global epidemiology of lung cancer. Ann Glob Health 85(1):8

Burley SK, Berman HM, Kleywegt GJ, Markley JL, Nakamura H, Velankar S (2017) Protein Data Bank (PDB): the single global macromolecular structure archive. Protein crystallography: methods and protocols, 627–641

Chaudhry GES, Zeenia, Sharifi-Rad J, Calina D (2024) Hispidulin: a promising anticancer agent and mechanistic breakthrough for targeted cancer therapy. Naunyn Schmiedebergs Arch Pharmacol 397(4):1919–1934

Choudhary N, Bawari S, Burcher JT, Sinha D, Tewari D, Bishayee A (2023) Targeting cell signaling pathways in lung cancer by bioactive phytocompounds. Cancers 15(15):3980

Citi V (2017) Mechanisms resistance analysis of inhibitors involved in the PI3K/Akt/mTOR pathway in vitro and in cftDNA collected from patients with breast tumors

Cummings BS, Schnellmann RG (2021) Measurement of cell death in mammalian cells. Curr Protoc 1(8):e210

Dai, Y., Sun, X., Li, B., Ma, H., Wu, P., Zhang, Y., … Wu, C. Z. (2021). The effect of hispidulin, a flavonoid from Salvia plebeia, on human nasopharyngeal carcinoma CNE-2Z cell proliferation, migration, invasion, and apoptosis. Molecules, 26(6), 1604.

da Silva CP, das Neves GM, Poser GLV, Eifler-Lima VL, Rates SMK (2023) In silico prediction of ADMET/drug-likeness properties of bioactive phloroglucinols from Hypericum genus. Med Chem 19(10):1002–1017

Eswaran A, Natarajan SR, Jayaraman S, Khan JM, Jasmine S, Veeraraghavan VP (2026) Jervine-induced suppression of triple-negative breast cancer (TNBC) cells growth through the regulation of Wnt signaling pathway-an in-silico and in-vitro approach. J Comput Aided Mol Des 40(1):57

Fatima, M., Iqubal, M. K., Iqubal, A., Kaur, H., Gilani, S. J., Rahman, M. H., … Rizwanullah,M. (2022). Current insight into the therapeutic potential of phytocompounds and their nanoparticle-based systems for effective management of lung cancer. Anti-Cancer Agents in Medicinal Chemistry (Formerly Current Medicinal Chemistry-Anti-Cancer Agents),22(4), 668–686.

Jiang N, Dai Q, Su X, Fu J, Feng X, Peng J (2020) Role of PI3K/AKT pathway in cancer: the framework of malignant behavior. Mol Biol Rep 47(6):4587–4629

Leiter A, Veluswamy RR, Wisnivesky JP (2023) The global burden of lung cancer: current status and future trends. Nat Rev Clin Oncol 20(9):624–639

Lv L, Zhang W, Li T, Jiang L, Lu X, Lin J (2020) Hispidulin exhibits potent anticancer activity in vitro and in vivo through activating ER stress in non-small-cell lung cancer cells. Oncol Rep 43(6):1995–2003

Mir SA, Bhat BA, Shenoy PS, Hamid L, Nisar N, Dar A, Ray P, Bader GN (2025) Naringenin inhibits cellular proliferation, arrests cell cycle and induces pro-apoptotic autophagy in MCF-7 breast cancer cells. J Cell Mol Med 29(15):e70747

Mir SA, Dar A, Hamid L, Nisar N, Malik JA, Ali T, Bader GN (2024) Flavonoids as promising molecules in the cancer therapy: An insight. Current Research in Pharmacology and Drug Discovery 6:100167

Mir, S. A., Dar, A., Alshehri, S. A., Wahab, S., Hamid, L., Almoyad, M. A. A., … Bader,G. N. (2023). Exploring the mTOR signalling pathway and its inhibitory scope in cancer.Pharmaceuticals, 16(7), 1004.

Natarajan SR, Krishnamoorthy R, Alshuniaber MA, Gatasheh MK, Rajagopal P, Veeraraghavan VP, Palanisamy CP, Jayaraman S (2025) KDM1A facilitates oncogenic potential in colorectal cancer progression through the activation of AXIN/GSK3β/β-catenin signaling pathways: evidence from integrated transcriptomics and in vitro studies. J Gene Med 27(11):e70053

Natarajan, S. R., Krishnamoorthy, R., Alshuniaber, M. A., Alsulami, T. S., Gatasheh,M. K., Rajagopal, P., … Jayaraman, S. (2025). ABCE1 facilitates tumour progression via aerobic glycolysis and inhibits cell death in human colorectal cancer cells through the p53 signalling pathway. Scientific Reports, 15(1), 24674.Xfxcfb

Natarajan, S. R., Krishnamoorthy, R., Alshuniaber, M. A., Al-Anazi, K. M., Farah,M. A., Rajagopal, P., … Jayaraman, S. (2024). Identification of FOXM1 as a novel protein biomarker and therapeutic target for colorectal cancer progression: Evidence from immune infiltration and bioinformatic analyses. International Journal of Biological Macromolecules, 282, 137201.

Patel K, Patel DK (2017) Medicinal importance, pharmacological activities, and analytical aspects of hispidulin: A concise report. J Tradit Complement Med 7(3):360–366

Velmurugan Y, Chakkarapani N, Natarajan SR, Jayaraman S, Madhukar H, Venkatachalam R (2025) PPI networking, in-vitro expression analysis, virtual screening, DFT, and molecular dynamics for identifying natural TNF-α inhibitors for rheumatoid arthritis. Mol Diversity, 1–20

Pushpanathan S, Gunasekaran A, Natarajan SR, Kannan K, Krishnan K (2025) Caffeic acid functionalized silver nanoparticles: a bionanoformulation and its assessment of cell cycle and in vitro cytotoxicity. Next Nanotechnology 7:100105

Safran, M., Dalah, I., Alexander, J., Rosen, N., Iny Stein, T., Shmoish, M., … Lancet,D. (2010). GeneCards Version 3: the human gene integrator. Database, 2010.

Schirrmacher V (2019) From chemotherapy to biological therapy: a review of novel concepts to reduce the side effects of systemic cancer treatment. Int J Oncol 54(2):407–419

Seetharaman PK, Liu B, Sivapunniyam A, Ramalingam KR, Ramalingam P, Natarajan SR (2025) Morin-Loaded Nanoalloy-Reduced Graphene Oxide Nanoplatforms for Synergetic Chemotherapy to Target Metastatic Triple-Negative Breast Cancer. ACS Appl Bio Mater 8(7):5699–5717

Sen A, Kumar K, Khan S, Pathak P, Singh A (2024) Current therapy in cancer: advances, challenges, and future directions. Asian J Nurs Educ Res 14(1):77–84

Shakoor B, Yaqoob N, Shafiq N, Bin Jardan YA, Nafidi HA, Bourhia M (2024) In silico ADME/Tox profiling of mushroom secondary metabolites. ChemSelect 9(4):e202304312

Siddiquee T, Bhaskaran NA, Nathani K, Sawarkar SP (2024) Empowering lung cancer treatment: Harnessing the potential of natural phytoconstituent-loaded nanoparticles. Phytother Res 38(8):3899–3920

Situmorang PC, Ilyas S, Nugraha SE, Syahputra RA, Nik Abd Rahman NMA (2024) Prospects of compounds of herbal plants as anticancer agents: a comprehensive review from molecular pathways. Front Pharmacol 15:1387866

ul Islam B, Suhail M, Khan MS, Ahmad A, Zughaibi TA, Husain FM, Tabrez S (2021) Flavonoids and PI3K/Akt/mTOR signaling cascade: a potential crosstalk in anticancer treatment. Curr Med Chem 28(39):8083–8097

Wang Y, Zhang T, He X (2023) Advances in the role of microRNAs associated with the PI3K/AKT signaling pathway in lung cancer. Front Oncol 13:1279822

Wu F, Li S, Zhang N, Huang W, Li X, Wang M, Bai D, Han B (2018) Hispidulin alleviates high-glucose-induced podocyte injury by regulating protective autophagy. Biomed Pharmacother 104:307–314

Zafar A, Khatoon S, Khan MJ, Abu J, Naeem A (2025) Advancements and limitations in traditional anti-cancer therapies: a comprehensive review of surgery, chemotherapy, radiation therapy, and hormonal therapy. Discov Oncol 16(1):607
Zughaibi TA, Suhail M, Tarique M, Tabrez S (2021) Targeting PI3K/Akt/mTOR pathway by different flavonoids: a cancer chemopreventive approach. Int J Mol Sci 22(22):12455

Authors and Affiliations

Selvam Rajendiran[1] · Sriram Prasath[1] · Nithya Ramesh[2] · Dhivya Murugesan[3] · Ramadurai Murugan[4] · Shobana Chandrasekar[5]

✉ Selvam Rajendiran
rselvam@dgvaishnavcollege.edu.in; arselvaam@gmail.com

Sriram Prasath
gsriramprasath@gmail.com; sriram@dgvaishnavcollege.edu.in

Nithya Ramesh
nithyar.biochem@spiher.ac.in

Dhivya Murugesan
dhivyadhanasekar@gmail.com

Ramadurai Murugan
drramadurai92@gmail.com

Shobana Chandrasekar
shobana.sls@velsuniv.ac.in

[1] Department of Biochemistry, Dwarakadoss Goverdhandoss Vaishnav College, Arumbakkam, Chennai, India

[2] Department of Biochemistry, St. Peters Institute of Higher Education and Research, Avadi, Chennai, India

[3] Department of Microbiology, Apollo Arts and Science College, Kanchipuram, India

[4] Center for Global Health Research, Saveetha Medical College and Hospitals, Saveetha Institute of Medical and Technical Sciences, Saveetha Nagar, Thandalam, Chennai 602 105, Tamilnadu, India

[5] Department of Biochemistry, School of Life Sciences, Vels Institute of Sciences, Technology and Advanced Studies (VISTAS), Pallavaram, Chennai, India